Tellus (1982), *34*, 540–544

The mass balance in diagnostic studies: an example of analysed and forecast data calculations

By HANNU SAVIJÄRVI[1], *European Centre for Medium Range Weather Forecasts, Shinfield Park, Reading, Berkshire RG2 9AX, England*

(Manuscript received November 27, 1981; in final form March 1, 1982)

ABSTRACT

The effects of non-zero mass balance, often encountered in diagnostic studies using observed data, are discussed for atmospheric energy budget equations written in sigma coordinates. An example of these effects is given by comparing the annual sensible heat budget over North America calculated from ECMWF grid point analyses and operational forecasts. The systematic height errors of the model appear as a local mass imbalance.

1. Introduction

Most diagnostic studies of atmospheric energetics require knowledge of the large-scale vertical velocity. A common way to estimate this variable is the kinematic method which uses the continuity equation in pressure coordinates. The horizontal wind divergence is integrated vertically starting from a given boundary value. The vertically integrated divergence should be nearly zero. However, if aerological wind data are used, this is not usually the case. The errors in the estimated divergence give rise to erroneous net divergence or convergence in the column. This erroneous net mass convergence must be removed if the diagnostics are to have any credibility. Various schemes to distribute the correction in the vertical have been suggested on an *ad hoc* basis. O'Brien (1970) reviewed the problem (which, from the mathematical point of view is the overspecification of a first-order differential equation with two boundary conditions) and suggested that the net mass balance correction be distributed linearly in pressure. Fig. 1 shows schematically a divergence profile and the results of using two common techniques of mass balance correction. Apart from these explicit correction methods, some studies (e.g. Perry, 1967; Savijärvi, 1977) have implicitly forced mass balance by fitting an analytic curve to the observed divergences with constraints that set its vertical integral to zero.

[1] Present affiliation: Department of Meteorology, University of Helsinki, Helsinki, Finland.

The purpose of the present paper is to discuss the mass balance in the σ-coordinate system and to give an example of the effect of the mass balance on the sensible heat budget equation. The σ coordinate data for the calculations are ECMWF initialized analyses, and forecasts made with the ECMWF grid point model. The analyses have a small or negligible local mass imbalance, while the systematic error of the numerical model appears as a local mass imbalance in the forecast data. This study is based on data used in a more detailed study of limited area atmospheric energy budgets (Savijärvi, 1981a), and is a condensed version of an internal report (Savijärvi, 1981b).

2. Mass balance in the σ-coordinate system

The σ-coordinate system is often used in numerical modelling because of the simple lower boundary condition. We will briefly consider the mass balance requirements in the σ-system. Here $\sigma = p/p_s$ is pressure normalized by the surface pressure.

If the equation of continuity in the σ-system is integrated vertically through the atmosphere from $\sigma = 0$ to $\sigma = 1$ and the boundary conditions $\dot{\sigma} = \mathrm{d}\sigma/\mathrm{d}t = 0$ at $\sigma = 0, 1$ are applied, the result is

$$\frac{\partial p_s}{\partial t} = -\int_0^1 \nabla_\sigma \cdot (p_s \mathbb{V})\, \mathrm{d}\sigma. \tag{1}$$

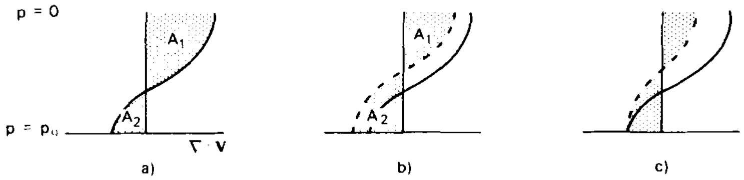

Fig. 1. (a) Schematic structure of a typical "observed" time mean large scale divergence profile with erroneous mass balance; $A_1 \neq A_2$. (b) Divergence profile with mass balance correction constant in pressure. (—— original data, ---- corrected data.) (c) Divergence profile with mass balance correction linear in pressure. Note that the shape of the profile is modifed. (—— original data, ---- corrected data.)

The time mean local pressure $\partial\bar{p}_s/\partial t$, where the overbar means a time average, is small at any point. The time and vertically averaged horizontal mass flux convergence $-\int_0^1 \nabla_\sigma \cdot (\overline{p_s \mathbb{V}})\, d\sigma$ must thus vanish in any air column.

However, if observed winds are used to estimate the time mean mass flux $\overline{p_s \mathbb{V}}$, the integrated horizontal mass flux convergence does not normally vanish. This implied local surface pressure change amounted to 15 mb day^{-1} over Europe in a recent study of three years of data (Alestalo, 1981).

Let $e(\sigma)$ be the error in the mass flux convergence estimate at each level

$$e(\sigma) = -\nabla_\sigma \cdot (\overline{p_s \mathbb{V}})_{\text{true}} + \nabla_\sigma \cdot (\overline{p_s \mathbb{V}})_{\text{observed}}, \tag{2}$$

and $\hat{e}$ its non-vanishing vertical mean:

$$\hat{e} = \int_0^1 e(\sigma)\, d\sigma = \int_0^1 \nabla_\sigma \cdot (\overline{p_s \mathbb{V}})_{\text{observed}}\, d\sigma. \tag{3}$$

Usually only $\hat{e}$ can be calculated, as $(\overline{p_s \mathbb{V}})_{\text{true}}$ is not known. The vertical distribution of $e(\sigma)$ may depend on data quality (O'Brien, 1970; Pedder, 1981).

The horizontal divergence of the time mean flux of any scalar variable s can be written as a sum of three terms

$$\nabla_\sigma \cdot (\overline{s p_s \mathbb{V}}) = \bar{s}\, \nabla_\sigma \cdot (\overline{p_s \mathbb{V}}) + \overline{p_s \mathbb{V}} \cdot \nabla_\sigma \bar{s} + \nabla_\sigma \cdot \overline{s'(p_s \mathbb{V})'}. \tag{4}$$

Use of eq. (2) to correct the time mean mass flux divergence after calculating (4) gives a better estimate of the observed s-flux divergence

$$\nabla_\sigma \cdot (\overline{s p_s \mathbb{V}})_{\text{true}} = \nabla_\sigma \cdot (\overline{s p_s \mathbb{V}})_{\text{obs}} - \bar{s}(\sigma) \cdot e(\sigma). \tag{5}$$

The mass balance correction is important if the first term on the right-hand side of (4) is dominant. If three-dimensional flux convergence is estimated from the horizontal wind data instead of the horizontal convergence only, the correction is $\bar{s}(\sigma) \cdot \hat{e}$ at each level because of the continuity equation in the σ-system.

Let us consider the flux form of the time mean sensible heat budget equation (6) as a specific example:

$$\frac{\partial}{\partial t} \overline{(c_p T p_s)} = -\nabla_\sigma \cdot \overline{(c_p T p_s \mathbb{V})} - \frac{\partial}{\partial \sigma} \overline{(c_p T p_s \dot{\sigma})} + \overline{p_s \alpha \omega} + \overline{p_s Q}. \tag{6}$$

The correction for the "observed" three-dimensional heat flux convergence is $c_p \bar{T}(\sigma)\, \hat{e}$. The large numerical values of $c_p T$ make the mass balance correction usually essential for reasonable results.

The erroneous mass balance is also present in the adiabatic heating term which can be written

$$p_s \alpha \omega = RT \mathbb{V} \cdot p_s - \frac{RT}{\sigma} \int_0^\sigma \nabla_\sigma \cdot (p_s \mathbb{V})\, d\sigma. \tag{7}$$

In the time-averaged data, the last term in (7) can be corrected with (2) giving an estimate for the "true" $\overline{p_s \alpha \omega}$

$$(\overline{p_s \alpha \omega})_{\text{true}} = (\overline{p_s \alpha \omega})_{\text{obs}} + \frac{R\bar{T}}{\sigma} \int_0^\sigma e(\sigma)\, d\sigma. \tag{8}$$

If the error is constant in the vertical, $e(\sigma) = \hat{e}$, then the mass balance correction for the adiabatic heating term is simply $R\bar{T}(\sigma)\hat{e}$.

The following diagnostic relation between the adiabatic heating $p_s \alpha \omega$, the kinetic energy generation $-p_s \mathbb{V} \cdot \nabla_\sigma \phi - RT \mathbb{V} \cdot \nabla_\sigma p_s$ and the pressure work term

$$\nabla_\sigma (\phi p_s \mathbb{V}) + \frac{\partial}{\partial \sigma} (\phi p_s \dot{\sigma}) + \frac{\partial}{\partial \sigma} \left(\phi \sigma \frac{\partial p_s}{\partial t} \right)$$

must also hold:

$$-p_s \mathbb{V} \cdot \nabla_\sigma \phi - RT \mathbb{V} \cdot \nabla_\sigma p_s + \nabla_\sigma \cdot (\phi p_s \mathbb{V})$$
$$+ \frac{\partial}{\partial \sigma}(\phi p_s \dot{\sigma}) + \frac{\partial}{\partial \sigma}\left(\phi \sigma \frac{\partial p_s}{\partial t}\right) + p_s \alpha \omega = 0. \qquad (9)$$

The correction for an estimate of the time-averaged three-dimensional divergence of geopotential flux is $-\bar{\phi}(\sigma)\hat{e}$. The remaining contribution in the pressure work term can be reformulated as

$$\frac{\partial}{\partial \sigma}\left(\phi \sigma \frac{\partial p_s}{\partial t}\right) = \sigma \frac{\partial}{\partial \sigma}\left(\phi \frac{\partial p_s}{\partial t}\right) + \phi \frac{\partial p_s}{\partial t}$$

$$= (-RT + \phi) \int_0^1 \nabla \cdot (p_s \mathbb{V})\, d\sigma. \qquad (10)$$

In the time-averaged data, a correction for this contribution is obviously $(-R\bar{T} + \bar{\phi})\hat{e}$. The correction for the complete pressure work term is thus $-R\bar{T}\hat{e}$. It is opposite to that of the adiabatic heating term. Consequently, it may be expected that the effect of the mass balance error is small in the estimate of the kinetic energy generation term, in spite of the fact that the generation is mainly determined by the divergent part of the wind.

3. Sensible heat budget calculations over North America

The annual budgets of kinetic energy, sensible heat and latent heat energy were published in Savijärvi (1981a) for three mid-latitude areas. They were based on ECMWF analyses and forecasts. The same data is used here to give an example of the mass balance in the forecast data in the σ-coordinate system. We concentrate here on the annual sensible heat budget (eq. (6)) averaged over the North American continent within latitudes 30–70° N and longitudes 80–140° W. The ECMWF analyses are made at pressure surfaces, then interpolated to 15 σ-levels and initialized (Temperton and Williamson, 1979). The initialized analyses and 3-day operational forecasts with the ECMWF grid-point model comprise the data for the time span December 1979–November 1980. The finite difference scheme for the various terms in eqs. (6) and (9) follows closely that of the ECMWF grid-point model in the staggered Arakawa C-scheme N48 grid. For details of the data and calculation methods, reference is made to Savijärvi (1981a).

The vertical profiles of the time and area averaged three-dimensional sensible heat flux convergence and the adiabatic heating terms (eq. 6) are shown in Fig. 2 both for the analysed data (4 analyses per day to remove the daily cycle) and for all 3-day ECMWF forecasts. The analyzed values indicate heat flux divergence and adiabatic heating. The forecast values have a similar vertical structure to the analyzed but they are shifted towards positive values. The shift (forecast minus analysis) is about 30 Wm^{-2} for the adiabatic heating term and about 110 Wm^{-2} for the heat flux convergence. The relation between these shifts is 0.27, near to $R/c_p = 0.286$, as might be expected from the discussion in Section 2.

The adiabatic heating, pressure work and kinetic energy generation terms are linked together by the diagnostic relation (9). They are shown in Fig. 3 as calculated from the analyzed data and 3-day forecasts. The shift between the forecast and analyzed profiles of the adiabatic heating is accompanied by a similar but opposite shift in the pressure work term. The kinetic energy generation term is nearly the same in the analyzed and forecast data, except in the boundary layer. It is also very similar to independent calculations from aerological data over the same area (Kung, 1967).

If another area or forecast ensemble is chosen, the shift between forecast and analyzed results varies but remains nearly constant in the vertical. This shift is thought to result from a change in the local mass balance in the ECMWF forecasts due to the systematic error of the model.

The structure of the systematic error varies from month to month but is in general negative (forecast heights are too low) over the eastern Atlantic and Pacific, having basically the same horizontal pattern at all levels. From day 2 to day 4 the 1000 mb heights typically increase over North America in the forecasts. Between day 6 and day 10 the 1000 mb height error becomes negative over the North American continent. This surface pressure drop is seen in the sensible heat budget as a shift in the opposite direction to that shown in Figs. 2 and 3.

If the difference between the sensible heat budget terms calculated from forecast and analyzed data

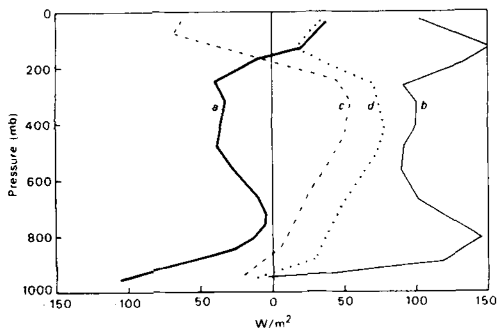

Fig. 2. The time and area-averaged heat budget terms over North America from ECMWF analyses (4 per day) and forecasts for day 3 during December 1979–November 1980. Units: Wm^{-2}. (a) 3-dimensional heat flux convergence from analyzed data. (b) 3-dimensional heat flux convergence from day 3 forecasts. (c) Adiabatic heating $\overline{p_s \alpha\omega/g}$ from analyzed data. (d) Adiabatic heating $\overline{p_s \alpha\omega/g}$ from day 3 forecasts.

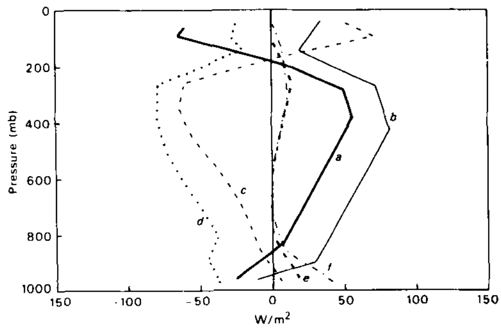

Fig. 3. The time and area averaged energy conversion terms over North America from ECMWF analyses (4 per day) and forecasts for day 3 during December 1979–November 1980. Units: Wm^{-2}. (a) $\overline{p_s \alpha\omega/g}$ from analyzed data. (b) $\overline{p_s \alpha\omega/g}$ from day 3 forecasts. (c) Pressure work from analyzed data. (d) Pressure work from day 3 forecasts. (e) Kinetic energy generation from analyzed data. (f) Kinetic energy generation from day 3 forecast data.

in Figs. 2 and 3 is entirely due to the change in local mass balance arising from the wind divergence due to the systematic error, the implied surface pressure increase is about 3 mb day^{-1}. This is a large but not unrealistic value.

Considering the analyzed values as "true", the forecast error can be defined as being the difference between the analyzed and forecast values. This forecast error in the sensible heat flux convergence is shown in Fig. 4. The dashed line gives the theoretical error curve $c_p\bar{T}(\sigma)\hat{e}$, using $\hat{e} = -\partial\bar{p}_s/\partial t = -3$ mb day^{-1}. The observed error profile and the theoretical error profile for the three-dimensional heat flux convergence are reasonably close, indicating that the major part of the forecast error is due to the mass balance effect, except in the stratosphere.

Fig. 5 shows the forecast error profile for the adiabatic heating, and the mass balance error curve $R\bar{T}(\sigma)\hat{e}$ suggested in Section 2. The error in the pressure work term is also shown together with the theoretical error $-R\bar{T}(\sigma)\hat{e}$. The forecast error is very close to the mass balance error in both cases except again in the stratosphere. For the adiabatic heating term, the theoretical error curve $R\bar{T}\hat{e}$ was based on a vertically constant divergence error structure (eq. (8)). The good fit between the forecast error and the theoretical curve indicates that the divergence error is almost independent of height in the forecast, which is in agreement with the largely barotropic nature of the ECMWF model systematic error.

4. Concluding remarks

The "raw" aerological wind data do not normally fulfil the requirement of local conservation of atmospheric mass. A recent study, Alestalo (1981), obtained a value of 15 mb day^{-1} for the surface pressure change using European rawinsonde data for three years. A value of 3 mb day^{-1} was found in the present study to explain the major part of the difference between the annual sensible heat budget terms calculated from ECMWF analysed and forecast data over North America. In the forecast data the mass balance is known to be distorted due to the spatially variable systematic error pattern of the ECMWF model.

The vertically uniform distribution of mass flux convergence error found here is in accordance with the barotropic nature of the ECMWF model systematic error (Derome, 1981). A similar systematic error pattern seems to be typical for some other short-range forecast models too (Bengtsson and Lange, 1981).

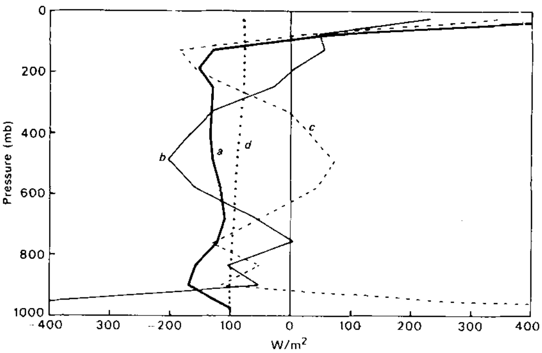

Fig. 4. The difference between analyzed and forecast sensible heat flux convergences over North America. Units: Wm^{-2}. (a) 3-dimensional flux convergence. (b) Horizontal flux convergence. (c) Vertical flux convergence. (d) $(c_p\overline{T}/g)\hat{e}$ where $\hat{e} = -\overline{\partial p_s/\partial t} = -3$ mb/day.

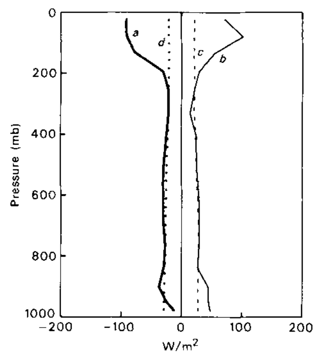

Fig. 5. The difference between analyzed and forecast pressure work and adiabatic heating over North America. Units: Wm^{-2}. (a) For adiabatic heating $\overline{p_s \alpha\omega/g}$. (b) For pressure work. (c) $-(R\overline{T}/g)\hat{e}$ where $\hat{e} = -\overline{\partial p_s/\partial t} = -3$ mb/day. (d) $+(R\overline{T}/g)\hat{e}$ where $\hat{e} = -\overline{\partial p_s/\partial t} = -3$ mb/day.

REFERENCES

Alestalo, M. 1981. The energy budget of the earth-atmosphere system in Europe. *Tellus 33*, 360–371.

Bengtsson, L. and Lange, A. 1981. *Results of the WMO/CAS NWP data study and intercomparison project for forecasts for the Northern Hemisphere in 1979–80.* WMO, Geneva.

Derome, J. 1981. On the average errors of an ensemble of forecasts. *Atmosphere-Ocean 19*, 103–127.

Kung, E. C. 1967. Diurnal and long-term variations of the kinetic energy generation and dissipation for a five-year period. *Mon. Wea. Rev. 95*, 593–606.

O'Brien J. 1970. Alternative solutions to the classical vertical velocity problem. *J. Appl. Meteorol. 9*, 197–203.

Pedder, M. 1981. On the errors of kinematic vertical motion estimation using bias adjustment procedures. *Mon. Wea. Rev. 109*, 1813–1816.

Perry, J. S. 1967. Long wave energy processes in the 1963 sudden stratospheric warming. *J. Atmos. Sci. 24*, 539–550.

Savijärvi, H. 1977. The interaction of the monthly mean flow and large-scale transient eddies in two different circulation types: vorticity and temperature balance. *Geophysica 14*, 207–229.

Savijärvi, H. 1981a. The energy budgets in North America, North Atlantic and Europe based on ECMWF analyses and forecasts. *Technical Report No. 27, ECMWF.* 31 pp., ECMWF, Reading, England.

Savijärvi, H, 1981b. On the mass balance correction in diagnostic studies. *Technical Memorandum No. 44, ECMWF.* 12 pp., ECMWF, Reading, England.

Temperton, C. and Williamson, D. 1979. Normal mode initialization for a multi-level grid point model. *Technical Report No. 11, ECMWF.* 99 pp., ECMWF, Reading, England.